Average Depths of Electron Penetration: Use as Characteristic Depths of Exposure

Valentin Lazurik[1], Vadim Moskvin[1] and Tatsuo Tabata[2]

[1]Radiation Physics Laboratory, Kharkov State University, P.O.Box 60, Kharkov, 310052, Ukraine

[2]RIAST, Osaka Prefecture University, 1-2 Gakuen-cho, Sakai, Osaka 599-8570, Japan

Abstract

The average depth of electron penetration is introduced as the physical quantity useful in electron beam irradiation. It is defined as the average of the maximum depths on the trajectories of electrons passing through finite, semi-infinite or infinite medium. The relation between the transmission coefficient as a function of slab thickness and the distribution of the maximum depths is analyzed, and a semiempirical equation to calculate the average depth of electron penetration is given for 0.1- to 50-MeV electrons incident on materials of atomic numbers from 4 to 92. It is shown that the quantity introduced is usable as the characteristic depths of energy and charge depositions in a target, and can possibly be generalized to the case of heterogeneous targets.

I. Introduction

The widespread use of electron beams in industrial applications these days motivates the development of simple methods for evaluating radiation effects on heterogeneous objects exposed to electrons. It is known that the effects caused by irradiation are generally determined by energy and charge depositions. When an object is exposed to an electron beam, radiation effects are observed in a finite spatial region in it. Studies of the geometrical characteristics of this region from the viewpoint of their usage to describe charge and energy depositions in the irradiated object are of interest for planning an experiment and for analyzing and interpreting experimental results.

For plane-parallel electron beams, it suffices to know a single parameter that represents an effective depth of the exposure region. The continuous slowing-down approximation (CSDA) range R_0, the extrapolated range R_{ex} and the projected range R_{pr} of electrons are frequently used as a characteristic depth in irradiated objects in electron-beam dosimetry [1]. The CSDA range does not take into account the scattering of electrons, and can therefore be used only as an upper limit to the depths of charge and energy depositions in a target. Although the extrapolated and projected ranges include the effects of multiple scattering, the procedures to determine these quantities have been introduced for homogeneous targets only. It is also to be noticed that the extrapolated range is an empirical quantity by definition. Thus, the ranges commonly used do not give information about features of electron penetration in heterogeneous objects.

The use of the projected range to describe the penetration of protons and alpha particles has been proposed by ICRU [2]. The detour factor as the measure of electron scattering in a target was implemented in electron-beam dosimetry by Harder [3] by the definition as the ratio of a characteristic depth, i.e., the extrapolated or projected range, to the CSDA range. On the basis of Monte Carlo data on the projected range, detour factors have been calculated for a wide region of the initial energy of electrons and varieties of target material [4]. The use of detour factor for scaling procedure in electron-beam dosimetry has been studied recently [5].

It should be noted that backscattering from deeper regions in a target can be significant for electrons, as distinct from heavy charged particles. Thus, a study of the absorption coefficients of electrons in a layer placed on the surface of a semi-infinite target shows that the electron scattering from surrounding materials in a heterogeneous object affects the absorption coefficient for a given material layer in the heterogeneous object [6]. Similarly, a study of charge deposition in slabs by primary electrons shows that its distribution considerably depends on the thickness of a target owing to change of the extent of the backscattering effect from deeper layers [7]. Thus, the projected range of electrons determined as the average of the depths of the track-end severely depends on the geometry of a target. To generalize its use for heterogeneous or inhomogeneous targets, the physical quantity for describing beam-exposure effects should be independent of the geometry.

The present work has been started by noticing that the largest depth an electron reaches during its motion in a target is in general different from the depth at which it is stopped. The goal of this present paper is to introduce a physical quantity related to the former depth and describe the results of studying it, for using it as a characteristic depth of exposure to an electron beam incident not only on homogeneous targets but also on inhomogeneous targets.

II. The Average Depth of Electron Penetration

A. Distributions of maximum depths of electron penetration and track-end points

To derive a characteristic depth of electron penetration in a target, we consider the behavior of electron trajectories and quantities determined by representative points on them. Let us define the maximum depth of electron penetration in a semi-infinite target as the largest depth an electron reaches during its motion in a target. One, and only one point on the electron trajectory represents this quantity. In general, this is not the track-end point of an electron trajectory.

0018-9499/98$10.00

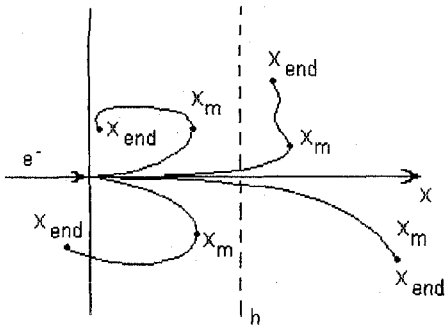

Figure 1: Electron trajectories in a target.

This is illustrated in Figure 1, where x_m is the maximum depth of electron penetration and x_{end} is the depth of track-end for a given trajectory.

For a set of electron trajectories, the distribution $D_m(x)$ of the maximum depths of electron penetration can be defined. Analogously to $D_m(x)$, the distribution $D_{end}(x)$ is defined as the depth-distribution of track-end points of electrons. This has also been called range distribution, range-straggling distribution or projected-range distribution by previous authors.

Next let us consider the properties of the distributions $D_m(x)$ and $D_{end}(x)$.

The distribution $D_m(x)$ has the following properties:

- A function $D_m(x)$ can be defined in the region of x from zero to infinity for both a semi-infinite and an infinite target.

$$D_m(x):\{x \in [0,\infty]\}. \qquad (1)$$

- The norm of the distribution $D_m(x)$ equals unity for a semi-infinite or an infinite target, i.e.,

$$\int_0^\infty D_m(x)dx = 1. \qquad (2)$$

- The distribution $D_m(x)$ does not depend appreciably on the geometry of a target, i.e., on its being semi-infinite or infinite (see solid curves in Figure 2; notice the last sentence of its caption).
- The distribution $D_m(x)$ in a finite target (a slab target) does not depends on the thickness h of the target, i.e., $D_m(x)$ for a slab target is equal to the part of $D_m(x)$ for $x<h$ in a semi-infinite or infinite target (see Figure 3; note the behavior of D_m near the down-stream interface as contrasted with that of D_{end}).
- The transmission coefficient $\eta(x)$ of electrons is uniquely determined by the distribution $D_m(x)$.

The following properties of the distribution $D_{end}(x)$ are different from those of $D_m(x)$:

- The norm of the distribution $D_{end}(x)$ is equal to unity only for an infinite target. It is equal to the absorption coefficient A for a semi-infinite target.

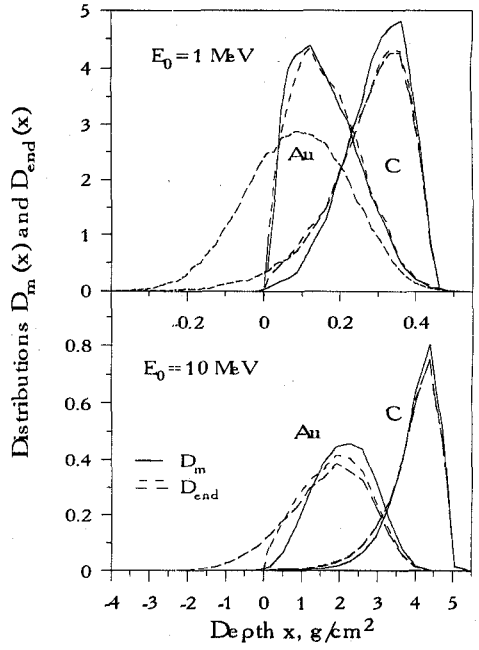

Figure 2: The distributions $D_m(x)$ of maximum depths of electron penetration (solid lines) and the distributions $D_{end}(x)$ of track-ends in infinite (dashed curves) and semi-infinite targets (dotted curves). $D_m(x)$ is plotted for semi-infinite targets, because the differences of the distributions computed for semi-infinite and infinite targets were less than 3%.

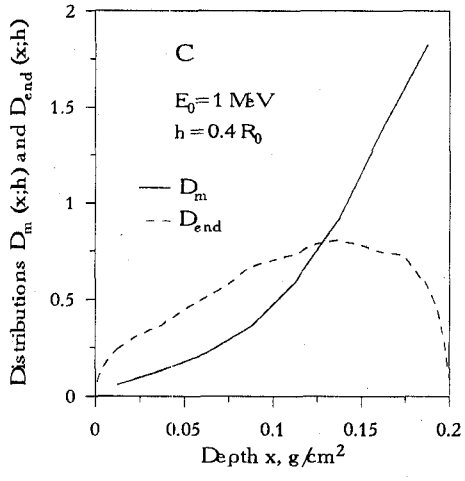

Figure 3: Distributions $D_m(x)$ (solid line) and $D_{end}(x)$ (dotted line) in a slab of thickness h irradiated by electrons of 1-MeV energy.

- The distribution $D_{end}(x)$ depends considerably on the geometry of a target (infinite, semi-infinite or finite targets; see dotted and dashed curves in Figure 2, and the dotted curve in Figure 3).

The curves plotted in Figures 2 and 3 were computed by Monte Carlo calculations for 50000 electron histories. The program unit used for tracing electrons has been described in [7]. The boundary effect on the distribution $D_{end}(x)$ was taken into account on the basis of the results presented in [8]. It is seen from Figures 2 and 3 that the distribution $D_{end}(x)$ depends strongly on the geometry of a target. This leads to differences in average depths defined by $D_{end}(x)$ for various

types of targets. For example, the projected ranges R_{pr} for an infinite target and a semi-infinite target can considerably be different (see Table 1). The difference is most significant for low-energy electrons incident on high atomic number targets, for which the boundary effect of a semi-infinite target is largest [8].

Table 1: The values of R_{pr}/R_0 for different geometrical configurations of a target.

		Absorber material	
Energy, MeV	Type of a target	C (Z=6)	Au (Z=79)
1 MeV	infinite	5.545E-1	1.151E-1
	semi-infinite	5.702E-1	2.131E-1
10 MeV	infinite	6.810E-1	2.769E-1
	semi-infinite	6.810E-1	3.102E-1

In contrast to $D_{end}(x)$, the distribution $D_m(x)$ shows negligible difference between the different geometrical configurations of a target as described before. Therefore, the average depth R_{av} of electron penetration for an infinite target is expected to be the same as the one for a semi-infinite target (this leads to the fact that R_{av} and R_{pr} for an infinite target can considerably be different). Further, the distribution $D_m(x)$ for a slab target is equal to part of the distribution $D_m(x)$ in a semi-infinite or an infinite target (Figure 3).

Thus, the distribution $D_m(x)$ of the maximum depths of electron penetration is independent of the geometry of a target. This feature of $D_m(x)$ is considered useful for generalizing the average depth of electron penetration R_{av} for the case of heterogeneous targets.

B. Semi-empirical equation to calculate the average depth of electron penetration.

Let us consider the last property mentioned of the distribution $D_m(x)$. Let the transmission coefficient $\eta(x)$ of electrons be measured in an "experiment" on the passage of electrons through a slab of a given thickness x. An electron is registered as the transmitted particle if its maximum depth x_m of penetration satisfies the condition $x_m >/= x$, and it is not registered as the transmitted particle if $x_m < x$ (see Figure 1). Therefore, we have

$$\eta(x) = \int_x^\infty D_m(x)dx . \tag{3}$$

Whence it follows that:

$$D_m(x) = -\left(\frac{d\eta(x)}{dx}\right). \tag{4}$$

Now we consider the average depth R_{av} of electron penetration in a semi-infinite target; it is defined by using $D_m(x)$ as follows:

$$R_{av} = \int_0^\infty xD_m(x)dx . \tag{5}$$

Substituting Equation (4) into Equation (3) and integrating the resulting equation, we obtain

$$R_{av} = \int_0^\infty \eta(x)dx . \tag{6}$$

The above equation uniquely expresses the relation between the average depth R_{av} in a semi-infinite target and the transmission coefficient $\eta(x)$ as a function of the slab thickness. Notice that Equation (6) has been derived without any additional assumption.

For $\eta(x)$, a semiempirical equation is available [9] (see Appendix). Substituting it into Equation (6), we obtain the following analytic expression for R_{av}:

$$R_{av} = \frac{1+\exp(-s_0)}{s_0+2}\ln\left[1+\exp(s_0)\right]R_{ex}, \tag{7}$$

where s_0 is the parameter depending on incident-electron energy and the atomic number of target material, and R_{ex} is the extrapolated range of incident electrons. For R_{ex}, semiempirical equations are also available [9,11].

The values of R_{av} were calculated for atomic numbers Z from 4 to 92 and incident-electrons energies E_0 from 0.1 to 50 MeV by the use of Equation (7), and the results are presented in the Table 2.

Comparison of the values of the average depth R_{av} of electron penetration with the conventional "ranges," i.e., the CSDA range R_0 (data taken from [10]) and extrapolated range R_{ex} [9] of electrons shows that R_{av} is less than either of these ranges. The ratios R_{av}/R_{ex} and R_{av}/R_0 strongly depend on both Z and E_0. In Figure 4, the ratio R_{av}/R_0 is plotted as a function of incident-electron energy (solid curves), showing an increase up to two times of its lowest values with increasing E_0 or decreasing Z.

The ratio R_{pr}/R_0 is also plotted in Figure 4 (dotted curves) to compare it with R_{av}/R_0. The values of R_{pr} were determined from the Monte Carlo results of $D_{end}(x)$ for semi-infinite targets [4].

From the definitions of R_{av} and R_{pr}, it is expected that R_{av} is always larger than R_{pr} for the same initial electron energy and the same material. The curves in Figure 4 mostly satisfy this expectation, but sometimes do not. This is considered to be caused by errors in the semi-empirical equations for $\eta(x)$ and R_{ex} used to calculate R_{av}. For fully understanding the behavior of R_{av}, accurate Monte Carlo results for this quantity are needed, but we have made the study of the general properties of R_{av}, as compared with R_{pr} and R_{ex}, as far as possible by using the presently available values. The results of such a study are given in the next section.

Table 2: The average depth R_{av} of electron penetration (in g/cm^2)

Energy	Absorber (Atomic number)						
E_0, MeV	Be(4)	C(6)	Al(13)	Cu(29)	Ag(47)	Au(79)	U(92)
0.1	1.176E-2	9.613E-3	8.256E-3	6.907E-3	6.012E-3	4.513E-3	3.790E-3
0.2	3.929E-2	3.123E-2	2.559E-2	2.059E-2	1.760E-2	1.292E-2	1.064E-2
0.5	1.638E-1	1.272E-1	1.005E-1	7.883E-2	6.723E-2	5.010E-2	4.135E-2
1	4.206E-1	3.253E-1	2.552E-1	1.993E-1	1.708E-1	1.313E-1	1.104E-1
2	9.894E-1	7.696E-1	6.094E-1	4.763E-1	4.078E-1	3.209E-1	2.760E-1
5	2.808E+0	2.213E+0	1.800E+0	1.437E+0	1.237E+0	9.931E-1	8.764E-1
10	5.858E+0	4.641E+0	3.817E+0	3.079E+0	2.664E+0	2.178E+0	1.959E+0
20	1.188E+1	9.409E+0	7.715E+0	6.155E+0	5.266E+0	4.278E+0	3.880E+0
50	2.941E+1	2.312E+1	1.848E+1	1.402E+1	1.149E+1	8.912E+0	8.044E+0

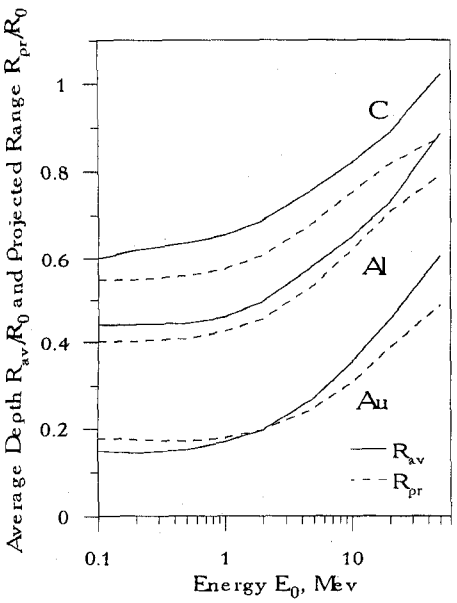

Figure 4: The average depth R_{av} of electron penetration (solid lines) and the projected range R_{pr} of electrons (dotted lines). R_{av} and R_{pr} are plotted as the ratio to CSDA range R_0 of electrons.

III. The Properties of Average Depth of Electron Penetration as the Characteristic Depth of Exposure

Let us consider the transmission coefficients $\eta(h)$ of electrons for a slab of thickness equal to R_{av} and R_{pr}. Figure 5 compares $\eta(R_{av})$ with $\eta(R_{pr})$ for various target materials and initial electron energies. This figure shows that the average depth R_{av} of electron penetration can be used as an approximate thickness of one-half attenuation of an electron beam. It is seen that the use of R_{av} as the thickness of one-half attenuation generally gives better approximation than the use of R_{pr}. Although the values of R_{av} and R_{pr} are rather close, the difference between $\eta(R_{av})$ and $\eta(R_{pr})$ are sometimes large. This is caused by a rapid decrease of $\eta(h)$ in the thickness region around R_{av} and R_{pr}. It should be noted that R_{ex} does not well characterize the average behavior of an electron beam in a target.

Considering the possible use of the average depth R_{av} of electron penetration to characterize the energy and charge deposition, we calculated the fractions of the energy and the charge deposited within the depths $x=R_{av}$ and $x=R_{pr}$ in a semi-infinite target. The data on energy and charge deposition in semi-infinite targets published in [12] were used for these calculations. The results obtained are shown in Figures 6 and 7.

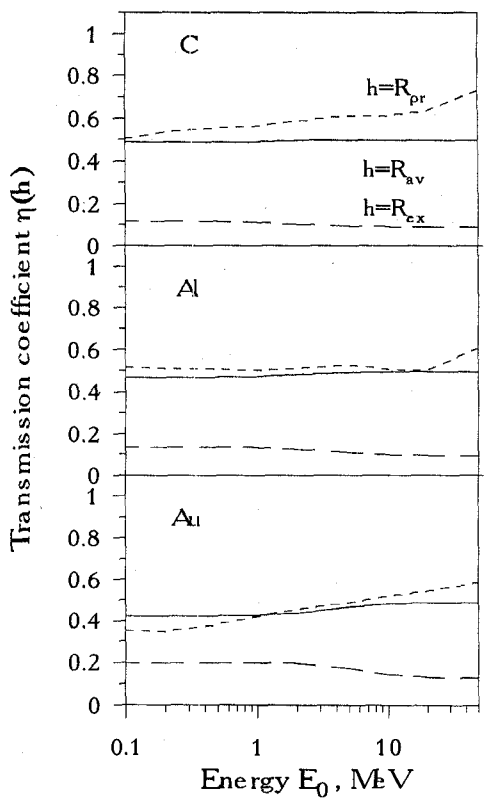

Figure 5: Transmission coefficient $\eta(h)$ for slabs of thickness h consisting of various materials as a function of incident energy E_0. Solid lines, $h = R_{pr}$; dotted lines, $h = R_{av}$; dashed lines, $h = R_{ex}$.

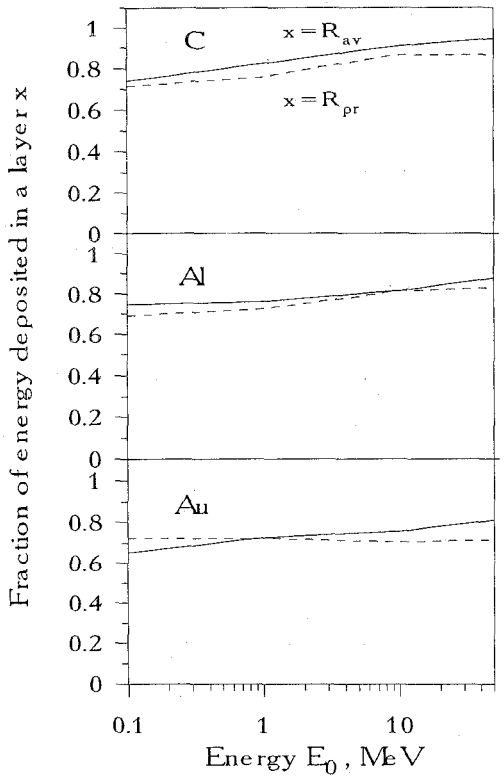

Figure 6: The fraction of the energy deposited within the depth x of a semi-infinite target as a function of incident energy E_0. Solid lines, $x=R_{av}$, dotted lines, $x=R_{pr}$.

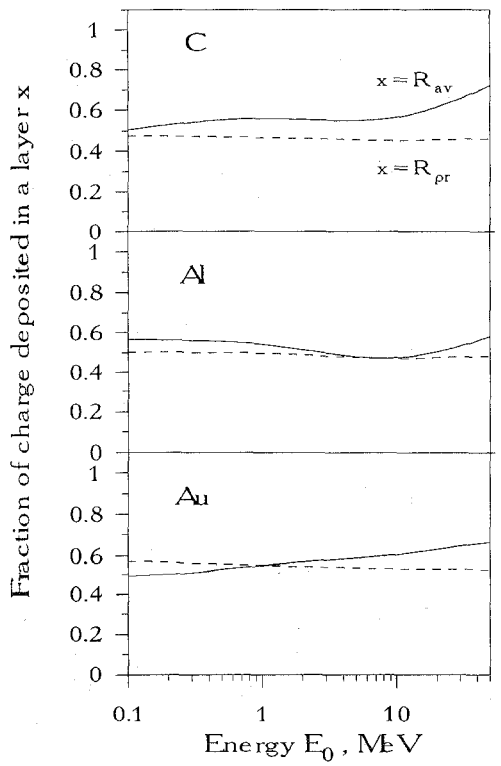

Figure 7: The fraction of the charge deposited within the depth x of a semi-infinite target as a function of incident energy E_0. Solid lines, $x=R_{av}$, dotted lines, $x=R_{pr}$.

The ratio of the energy deposition down to the depth of R_{av} or R_{pr} to the total energy deposition in the target has been found to be $0.8+/-\delta_1$, where δ_1 equals 0.08, and the ratio is roughly a constant within an accuracy of 20% (see Figure 6). Thus both the average depth R_{av} of electron penetration and the projected range R_{pr} can be used as the characteristic depth of energy deposition or exposure to electron beams in semi-infinite targets.

The use of the characteristic depth R_{av} for the estimation of energy deposition is illustrated in Figure 8. Down to the depth R_{av}, the effective energy $D_{ef}(x)dx$ deposited at a layer of thickness dx at the depth x can be represented in a good approximation by

$$D_{ef}(x)dx = \frac{0.8E_a}{R_{av}}dx, \qquad (8)$$

where E_a is the primary-electron energy deposited in a semi-infinite target.

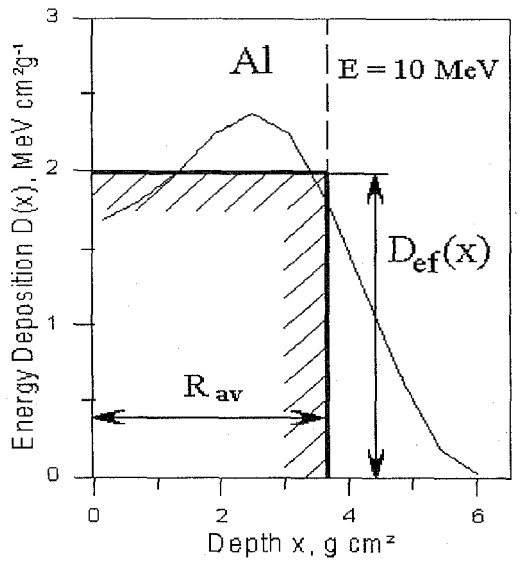

Figure 8: The effective energy deposition $D_{ef}(x)$ down to the depth of R_{av} and the profile $D(x)$ of energy deposition.

Because R_{av} is numerically close to the projected range R_{pr} determined from the charge-deposition distribution by primary electrons, it is expected that the former can also be used to characterize the charge deposition. Figure 7 shows that R_{av} rather well describes the depth within which approximately half the total charge is deposited, confirming the above expectation.

Thus, the present results have shown that the average depth R_{av} of electron penetration can be used as the characteristic depth of exposure to electrons in homogeneous semi-infinite targets. In contrast to the projected range R_{pr}, the definition of R_{av} can be generalized to the case of slab and heterogeneous targets. Therefore, the latter quantity would be more useful than the former for application purposes.

IV. REFERENCES

[1] ICRU, Radiation dosimetry: electron beams with energies between 1 and 50 MeV, ICRU Report 35, Bethesda, MD, 1984.

[2] ICRU, Stopping powers and ranges for protons and alpha particles, ICRU Report 49, Bethesda, MD, 1993.

[3] D. Harder, Some general results from the transport theory of electron absorption, *Proc. 2nd Symp. on Microdosimetry, Stressa, Italy 1969*, ed. H. G. Ebert, Brussels, Euratom, pp. 567-593, 1970.

[4] T. Tabata, P. Andreo, K. Shinoda and R. Ito, "Range distributions and projected ranges of 0.1- to 100 MeV electrons in elemental absorbers", *Nucl. Instrum. and Methods B*, vol. 108, pp. 11-17, 1996.

[5] J. M. Fernández-Varea, P. Andreo and T. Tabata, "Detour factors in water and plastic phantoms and their use for range and depth scaling in electron-beam dosimetry", *Phys. Med. Biol.* vol. 41, pp. 1119-1139, 1996.

[6] V. Lazurik and V. Moskvin, "Absorption of fast electrons in thin slabs", *IEEE Trans. Nucl. Sci.*, vol. 44, No.3, pp. 1070-1075, June 1997.

[7] V. Lazurik and V. Moskvin, "Monte Carlo calculation of charge deposition depth profile in slab irradiated by electrons", *Nucl. Instr. and Meth. B.* vol. 108, pp. 276-282, 1996.

[8] V. Lazurik and V. Moskvin, "Charge deposition distributions in targets irradiated by electrons", *IEEE Trans. Nucl. Sci.*, vol. 44, No.3, pp. 1065-1069, June 1997.

[9] T. Tabata and R. Ito, "A generalized empirical equation for the transmission coefficient of electrons", *Nucl. Instrum. and Methods*, vol. 127, pp. 429-434, 1975

[10] ICRU, Stopping powers for electrons and positrons, ICRU Report 37, Bethesda, MD, 1984.

[11] T. Tabata, "Theoretical Evaluation of Absorbed Doses in Materials by Low-Energy Electron Beams: A Short Review", *Bulletin of University of Osaka Prefect., Ser.A*, Vol. 1, pp. 41-46, 1995.

[12] P. Andreo, T. Tabata and R. Ito, "Tables of Charge and Energy Deposition Distributions in Elemental Materials Irradiated by Plane Parallel Electron Beams with Energies between 0.1 and 100 MeV", *Technical Report 1, RIAST*, University of Osaka Prefecture, 1992.

V. APPENDIX

The semiempirical equations for $\eta(x)$, s_0 and R_{ex} developed in [9] are given

$$\eta(x) = \frac{1+\exp(-s_0)}{1+\exp\left[(s_0+2)\frac{x}{R_{ex}} - s_0\right]}, \tag{9}$$

$$s_0 = a_1 \exp\left[-\frac{a_2}{1+a_3\tau_0{}^{a_4}}\right], \tag{10}$$

where:

$$a_1 = \frac{10.63}{Z^{0.232}}, \tag{11}$$

$$a_2 = 0.22Z^{0.463}, \tag{12}$$

$$a_3 = 0.042, \tag{13}$$

$$a_4 = 1.86. \tag{14}$$

$$R_{ex} = c_1\left[\frac{1}{c_2}\ln(1+c_2\tau_0) - \frac{c_3\tau_0}{1+c_4\tau_0{}^{c_5}}\right], \tag{15}$$

where:

$$c_1 = \frac{0.2335A}{Z^{1.209}}\ \text{g/cm}^2, \tag{16}$$

$$c_2 = 1.78\times10^{-4}Z, \tag{17}$$

$$c_3 = 0.9891 - 3.01\times10^{-4}Z, \tag{18}$$

$$c_4 = 1.468 - 1.180\times10^{-2}Z, \tag{19}$$

$$c_5 = \frac{1.232}{Z^{0.109}}. \tag{20}$$

where $\tau_0=E_0/mc^2$; mc^2 is the rest energy of the electron; Z is the atomic number and A is the atomic weight of the absorber.